

Chapter 4

Three Experiments



To set up the remainder of this article let us pose three problems. They incorporate various issues arising from basic analysis to simulation to applied modelling. Their seemingly ambiguous dynamics expose remarkably well our current state of knowledge concerning the robustness of nonsmooth models. The problems are: a classic example of ambiguity from seminal texts; a two-gene regulatory system with seemingly ambiguous activation of genes; and an investment game where players' seemingly steady behaviour destabilizes a company's trading.

To solve these systems we must decide how to handle a discontinuous term like $\text{step}(\sigma)$, in particular, to decide what value to assign to $\text{step}(0)$. We can do this in a number of different ways, which we call *implementations*. We will make a preliminary definition of these here, to be refined in Chap. 5, along with six *test implementations* that we use for simulations in this article.

Definition 4.1. Given a system in which a parameter switches according to an ideal rule $v = \text{step}(\sigma)$, we define an **implementation** of the switch as a rule that forms a transition layer $|\sigma| \leq \varepsilon$ and determines the selection of modes $v = 0$ and $v = 1$ within it. In $|\sigma| > \varepsilon$ the modes are assigned uniquely according to $v = \text{step}(\sigma)$. For our purposes here this can involve one or more of the following six *test implementations*:

- *smoothing*—the switch is enacted by replacing v with a smooth monotonic function $\phi^\varepsilon(\sigma)$ satisfying $\phi^\varepsilon(\sigma) \rightarrow \text{step}(\sigma)$ as $\varepsilon \rightarrow 0$;
- *hysteresis*—the switch is enacted by mapping $v : \{0 \text{ or } 1\} \mapsto 1$ at $\sigma = +\varepsilon$, and $v : \{0 \text{ or } 1\} \mapsto 0$ at $\sigma = -\varepsilon$;
- *time delay*—the switch is enacted by mapping $v : 0 \leftrightarrow 1$ a time $\delta t = \varepsilon$ after crossing $\sigma = 0$, that is, $v = \text{step}(\sigma(t - \varepsilon))$;
- *time stepping*—the rule $v = \text{step}(\sigma)$ is evaluated only at discrete time steps $\delta t = \varepsilon$;
- *noisy time delay*—as in time delay, but with the delay chosen randomly between $0 < \delta t < \varepsilon$ each time a switch occurs;
- *spatial noise*—as in smoothing, but the state is also perturbed by adding random translations of a size smaller than some $\kappa \ll 1$ at time steps $\delta t = \alpha \ll 1$.

In each case ε is a small positive constant. To consider a system with multiple switches we introduce parameters $\nu_i = \text{step}(\sigma_i)$ for $i = 1, 2, \dots$, which switch at thresholds $\sigma_i = 0$, and in the case of smoothing, hysteresis, or time delay, involve different small quantities ε_i , $i = 1, 2, \dots$ associated with each threshold.

We have expressed the switch in terms of $\nu = \text{step}(\sigma)$ without loss of generality, and could instead have used any other discontinuous function, such as $\lambda = \text{sign}(\sigma)$ for which the implementations follow directly via the relation $\lambda = 2\nu - 1$.

Of course one may consider other implementations besides those above, for instance perturbations that increase the dimension of the system. The list above will be sufficient for this exploratory study, but there are certainly extensions to be made, and perhaps a more general but less explicit formulation will be found. We will not consider the implementation that is provided by using event detection in computational software, because this requires an additional decision to be made of what dynamics to impose on $\sigma = 0$, a decision we are not yet ready to make.

4.1 Filippov's Convexity Paradox

The following problem is adapted from one posed by Filippov in section 7 example 134 of [51]. Consider a planar system

$$\begin{pmatrix} \dot{x} \\ \dot{y} \end{pmatrix} = \begin{pmatrix} -\frac{1}{2} - \lambda \\ \frac{1}{3} + \lambda^3 \end{pmatrix}, \quad (4.1)$$

where $\lambda = \text{sign}(x)$, and assuming $\lambda \in [-1, +1]$ when $x = 0$. Whatever the flow in this system, the vector field for $x \neq 0$ simply points towards $x = 0$, so the flow is attracted to the discontinuity at $x = 0$ and must remain there. All that remains is to find its speed of motion along $x = 0$.

In Fig. 4.1(i–vi) we simulate (4.1) using the test implementations of the switch set out in Definition 4.1. Smoothing the discontinuity (and then simulating using some standard numerical integration package), we obtain the trajectory in portrait (i) of Fig. 4.1. Simply discretizing Eqs. (4.1) instead gives the portrait (ii). Introducing hysteresis or delay in the switch yields similarly (iii)–(iv), while a noisy delay yields (v). In (vi) we see two examples of what happens with a combination of such effects, as we smooth Eqs. eq. (4.1), discretize them, and then introduce spatial noise: for small enough noise the simulation agrees with (ii–v), for large noise it agrees with (i), up to random variations. The sizes of these perturbations are described in the figure caption.

All show motion along the discontinuity threshold, but some result in motion upward at a speed $\dot{y} \approx 5/24$, while others evolve downward at a speed $\dot{y} \approx -1/6$ (we will see why these specific values of the speed arise). Implemented with noise, either type of solution can be obtained for sufficiently large or small amplitude of random perturbations.

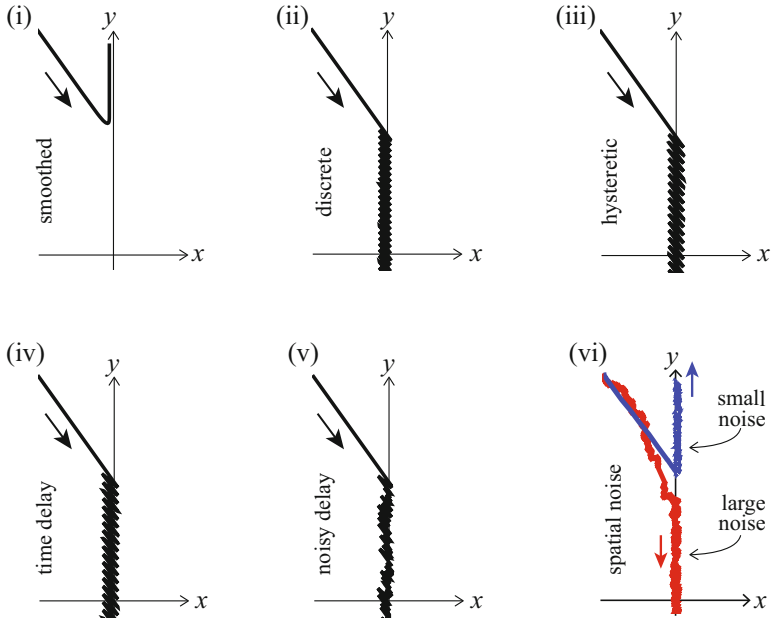


Fig. 4.1 The system from Fig. 7.1 simulated from a point in $x < 0$, where the switch implementation is: (i) smooth, (ii) time stepping, (iii) hysteretic, (iv) time-delayed, (v) with a noisy time delay, or (vi) with spatial noise (large or small noise, slightly displaced for clarity). Simulated using (4.1) and Definition 4.1 with $\varepsilon = 0.1$. In (v) we use $\kappa = \alpha = 0.1$ for small noise and $\kappa = 0.2$, $\alpha = 0.01$, for large noise. Similar results are obtained for any initial conditions and any choice of smoothing function

This was essentially this problem posed by Filippov, but considering only an idealized system (i.e., not considering such implementations), to highlight issues of uniqueness of solutions to (4.1). Filippov's theory, taken as a whole, allows for all of the different outcomes in Fig. 4.1, but his most commonly accepted concept of 'sliding' along the discontinuity threshold favours the outcomes in (ii)–(v), in contradiction to the outcome of smoothing in (i).

Given such a simple system as (4.1), the contrasting results in Fig. 4.1 reveal somewhat of a conceptual pickle in the state of understanding of nonsmooth dynamical theory, one that will become more pronounced over the next couple of examples. Distinguishing between the different possibilities and when to expect them is vital for applications, and moreover is achievable given recent advances, such as [18, 79, 83, 129, 131, 132]. These have provided hints of conditions to distinguish between alternative behaviours, but rigorous results are piecemeal, lengthy, and technical, even in the simplest cases when one smooths a discontinuity [111] or adds hysteresis [18].

One might be concerned that we can hope at all to develop a serious theory of nonsmooth models in the light of such contrary results. We will show that these are each correct and reconcilable within definite perturbative contexts. We will also show that these pale against other indeterminacies that have come to light in

recent years, not limited to speed or direction of motion along the threshold, but also whether solutions evolve along the threshold at all or simply cross through it.

4.2 On or Off Genes

An example studied in [117] concerns a model of two genes responsible for producing proteins with concentrations x_i , which obey

$$\begin{pmatrix} \dot{x}_1 \\ \dot{x}_2 \end{pmatrix} = \begin{pmatrix} v_1 + v_2 - 2v_1v_2 - \gamma_1x_1 \\ 1 - v_1v_2 - \gamma_2x_2 \end{pmatrix} := \mathbf{f}^{v_1v_2}(x_1, x_2), \quad (4.2)$$

where $v_i = \text{step}(x_i - \theta_i)$ for some positive constants $\theta_1, \theta_2, \gamma_1, \gamma_2$, for which we assume $0 < \gamma_i\theta_i < 1$. The switching of each v_i models the (de-)activation of the i^{th} protein production as its concentration x_i passes a threshold value θ_i , as we introduced in Sect. 1.3. It will be convenient to express the right-hand side as a planar vector field $\mathbf{f}^{v_1v_2}(x_1, x_2)$, as sketched in Fig. 4.2(top-left).

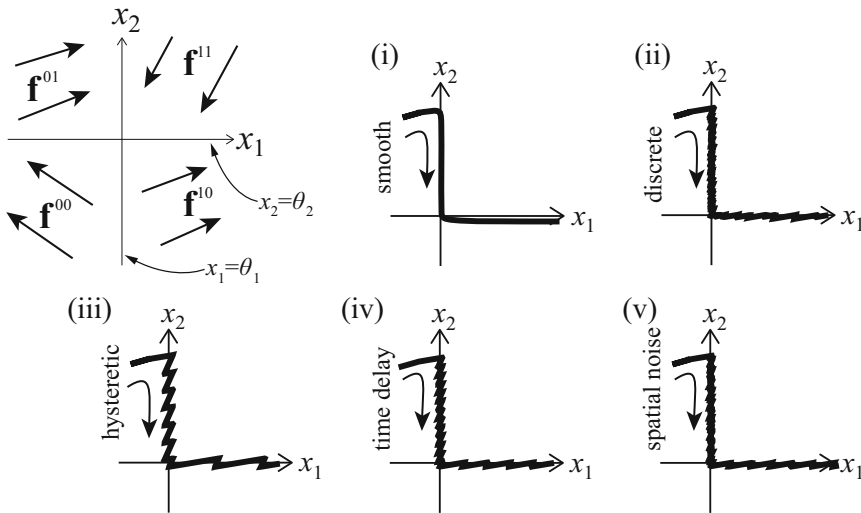


Fig. 4.2 A two-gene system switching between four modes (top-left), and its flow simulated from a point in $x_1 < \theta_1, x_2 < \theta_2$, in (i–v). The solution evolves onto the discontinuity threshold $x_1 = \theta_1$, and proceeds onto the threshold $x_2 = \theta_2$, where it then remains approximately. The switch is modelled as: (i) smooth (substituting v_i with $v_i = x_i^{1/\varepsilon_i} / (\theta_i^{1/\varepsilon_i} + x_i^{1/\varepsilon_i})$ for small constants ε_i), (ii) time stepping, (iii) hysteretic, (iv) time-delayed, or (v) with a noisy time delay. Simulated from (4.2) for parameters $\theta_1 = \theta_2 = 1, \gamma_2 = 0.9, \gamma_1 = 0.4$, and implemented with $\varepsilon_1 = \varepsilon_2 = \alpha = \kappa = 0.2$ (as described in Definition 4.1)

The range of behaviours that are possible at the discontinuity thresholds is less obvious than in Sect. 4.1. Clearly the half-lines $x_1 = \theta_1, x_2 > \theta_2$, and $x_2 = \theta_2, x_1 > \theta_1$ are attracting, so motion can only proceed along the thresholds there, and

solutions can only escape those portions at the point $x_1 - \theta_1 = x_2 - \theta_2 = 0$ where they intersect. Elsewhere, on $x_1 = \theta_1, x_2 > \theta_2$, and $x_2 = \theta_2, x_1 > \theta_1$, it can be shown that solutions cross these thresholds transversally (see [82, 117]). Let us focus solely on what happens at $x_1 - \theta_1 = x_2 - \theta_2 = 0$ after motion along $x_1 - \theta_1 = 0 < x_2 - \theta_2$.

Similarly to Sect. 4.1 we simulate the system by implementing the two discontinuities in the manner of Definition 4.1. The results are shown in Fig. 4.2 for parameter values given in the caption. In all cases the solution evolves onto the threshold $x_1 = \theta_1, x_2 > \theta_2$, travels downward until reaching the intersection $x_1 - \theta_1 = x_2 - \theta_2 = 0$, and ‘rounds the corner’ onto the threshold $x_2 = \theta_2, x_1 > \theta_1$. (In fact the solution continues towards an equilibrium state at $x_1 \approx \theta_2\gamma_2/\gamma_1, x_2 \approx \theta_2$, not shown). The outcome appears to be robust to the method of implementation.

For a different set of parameters, however, we obtain the contradictory behaviours shown in Fig. 4.3. This is despite the vector fields outside the discontinuity thresholds $x_i = \theta_i$ being qualitatively unchanged. Implemented by smoothing, time stepping, or time delay, the solution now sticks upon reaching $x_1 - \theta_1 = x_2 - \theta_2 = 0$. With hysteresis the solution rounds the corner as before; however, isolated param-

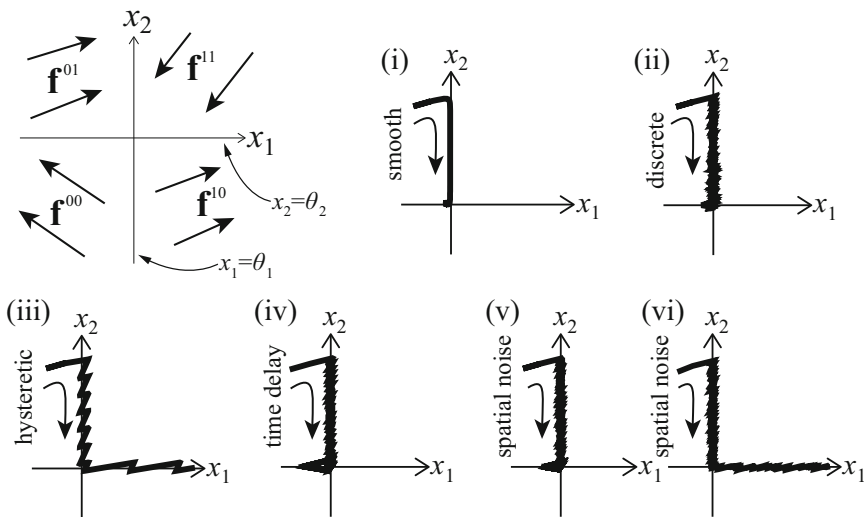


Fig. 4.3 As in Fig. 4.2 except $\gamma_1 = 0.6$. The solution evolves onto the discontinuity threshold $x_1 = \theta_1$, along which it evolves onto $x_1 = \theta_1, x_2 = \theta_2$, where it then remains (approximately), for all implementations except the last—noisy solutions can either stick (v) for $\kappa \gg 0.02$, or round the corner (vi) for $\kappa \ll 0.02$, while near $\kappa \approx 0.02$ intermittency is seen, with repeated simulations showing either behaviour

eter values $\varepsilon_1 \neq \varepsilon_2$ can be found for which the hysteretic solution does stick to $x_1 - \theta_1 \approx x_2 - \theta_2 \approx 0$, for example, $\varepsilon_1 = 0.01, \varepsilon_2 = 0.02$ (not shown). Implementing with noise we are able to see both behaviours: sticking at the origin for small enough noise, rounding the corner for larger noise, and in between, an intermittency whereby repeated simulations may show either behaviour due to the randomness of perturbations.

These contrary results can be explained, and a context to do so is provided in the following sections. In short they hinge on the existence or not of an attractor at $x_1 - \theta_1 = x_2 - \theta_2 = 0$ and its stability under perturbation. Re-considering the literature in the light of the results above, one recognizes hints towards them in studies such as [117] and [2]. In [117] the dynamics at the threshold is studied assuming the quantities v_i are actually smooth ‘Hill’ functions, $\phi_i^{\varepsilon_i}(x_i) = x_i^{1/\varepsilon_i} / (\theta_i^{1/\varepsilon_i} + x_i^{1/\varepsilon_i})$, which tend to $\text{step}(x_i - \theta_i)$ as $\varepsilon_i \rightarrow 0$ [70].

Even if solutions stick robustly to the intersection $x_1 - \theta_1 = x_2 - \theta_2 = 0$, their fate might still not be obvious, as the following example shows.

4.3 Jittery Investments

Consider a game in which two players each buy and sell stocks in a company, denoting the amounts they own as x_1 and x_2 , measured relative to some desirable asset level $x_i = 0$, and let the stocks owned by the company itself be z . The system and phenomenon we describe below extend readily to more players and companies. The rules we assign will be simple to illustrate the mathematical phenomenon at work, but there is very little special about how they are chosen, and one could certainly improve the game with more realistic trading rules and other players with more defined roles without destroying the phenomenon.

Let x_i purchase stocks at a rate c , and sell them back to the company at a rate $-\gamma_i$ only if $x_i > 0$, so

$$\dot{x}_i = \begin{cases} c - \gamma_i & \text{if } x_i > 0, \\ c & \text{if } x_i < 0. \end{cases}$$

If $0 < c < \gamma_i$, then each player is attracted towards their respective threshold $x_i = 0$.

Let us express this in terms of a switching multiplier $v_i = \text{step}(x_i)$ simply as $\dot{x}_i = c - \gamma_i v_i$. Nonlinear terms can be used to introduce strategic choices, for example, we may add an increased rate of buying ρ_i in response to competition from other players in the form

$$\dot{x}_i = c - \gamma_i v_i - \rho_i v_1 v_2, \quad i = 1, 2. \quad (4.3)$$

The company’s level of self-owned stocks is then fed and depleted by the two players, giving

$$\dot{z} = -2c + \gamma_1 v_1 + \gamma_2 v_2 - \rho_{11} v_1 v_2 + \rho_{00} (1 - v_1)(1 - v_2), \quad (4.4)$$

where we also give the company its own strategic terms, namely an increase in selling off to other parties at rate ρ_{11} if both players are selling at the same time, or an increase in buying back shares from other parties at rate ρ_{00} if both players are buying at the same time.

We will denote the right-hand side of the three-dimensional vector field defined by (4.3)–(4.4) as $\mathbf{f}^{v_1 v_2}$, so

$$\begin{aligned}
 (\dot{x}_1, \dot{x}_2, \dot{z}) &= \mathbf{f}^{v_1 v_2} \\
 &:= \left(c - \gamma_1 v_1 - \rho_1 v_1 v_2, \quad c - \gamma_2 v_2 - \rho_2 v_1 v_2, \right. \\
 &\quad \left. - 2c + \gamma_1 v_1 + \gamma_2 v_2 - \rho_{11} v_1 v_2 + \rho_{00}(1 - v_1)(1 - v_2) \right),
 \end{aligned}
 \tag{4.5}$$

and we assume $\gamma_i + \rho_i > c > 0$ for $i = 1, 2$.

The piecewise-constant vector field is sketched in the (x_1, x_2) plane in Fig. 4.4, and again appears extremely simple: the flow evolves onto the thresholds $x_1 = 0$ and $x_2 = 0$, where it must remain. The simulations in Fig. 4.4 reveal that for any implementation (i)–(v), solutions evolve towards the intersection $x_1 = x_2 = 0$ and remain there for all later times.

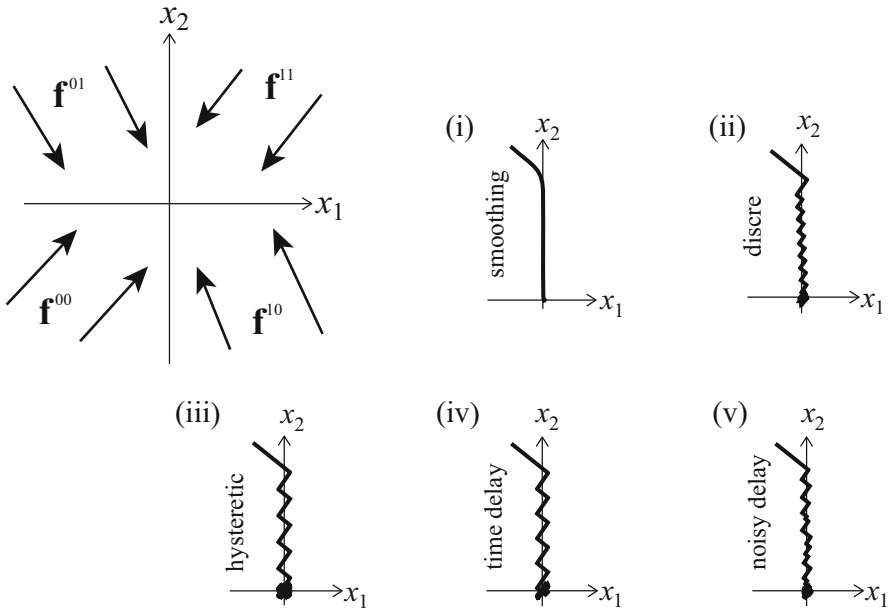


Fig. 4.4 An investment game with four modes. The vector field is sketched (top-left), and its flow is simulated in (i)–(v) from a point in $x_1 < 0 < x_2$ by the different implementations from Definition 4.1. The solution evolves onto the discontinuity threshold $x_1 = 0$, then towards the intersection with the second discontinuity threshold $x_2 = 0$, where it remains (approximately), regardless of implementation, and for any parameter values (given $\gamma_i + \rho_i > c > 0$ for $i = 1, 2$)

Thereafter only the company’s holdings, z , may fluctuate, so we must ask how this is affected by the investment dynamics of the two players. As in Sects. 4.1 and

4.2, our task reduces to determining the speed of motion along the discontinuity threshold, in this case the rate of change of z on $x_1 = x_2 = 0$.

We find a rather different phenomenon, with more erratic variability, than in Sects. 4.1 and 4.2.

The result of simulations for the implementations using smoothing, hysteresis, time delay, or time stepping is shown in Fig. 4.5, for two different games (i.e., two sets of parameters). The speed \dot{z} is plotted for different ratios of the implementation parameters ε_i , which are defined as $(\varepsilon_1, \varepsilon_2) = \varepsilon(\cos \frac{\omega\pi}{2}, \sin \frac{\omega\pi}{2})$. Note for time stepping there is only one ε parameter (the time step) so the graph is a horizontal line.

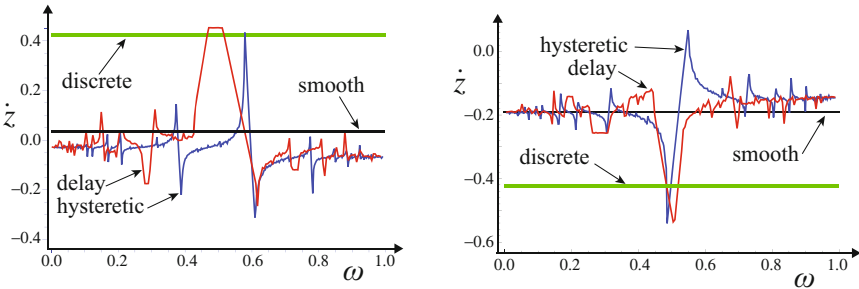


Fig. 4.5 The company's rate of change \dot{z} for noise-free implementations of the investment game. Left: using $c = 1$, $\gamma_1 = 1.4$, $\gamma_2 = 1.8$, $\rho_1 = 0.5$, $\rho_2 = 0.5$, $\rho_{11} = 1$, $\rho_{00} = 3$. Right: using $c = 0.5$, $\gamma_1 = 1.1$, $\gamma_2 = 1.4$, $\rho_1 = 0.4$, $\rho_2 = 0$, $\rho_{11} = 2$, $\rho_{00} = 0.4$

First note, alarmingly, how the two different approaches we might favour in computer simulations—time stepping or smoothing—give markedly different rates of change for z . Note also how the delayed or hysteretic implementations depend erratically on the relative size of delay/hysteresis across $x_1 = 0$ and $x_2 = 0$, i.e., the ratio ω .

The two different games in Fig. 4.5 exhibit markedly different behaviour. The behaviour outside $x_1 = x_2 = 0$ does not change significantly between these parameter values, remaining always pointing 'inwards' towards the origin. Despite this the speed of motion along $x_1 = x_2 = 0$ changes, both between the two parameter sets, and as we vary the implementation parameter $\varepsilon_2/\varepsilon_1 = \tan \frac{\omega\pi}{2}$. We could plot similar graphs with any of the parameters c , γ_i , ρ_i , on the horizontal axis in place of ω , and obtain similarly erratic curves.

The noisy implementations are missing from Fig. 4.5. The same two games are implemented with noisy delay or spatial noise (see Definition 4.1) in Fig. 4.6. Counterintuitively, the outcome is less erratic in the noisy conditions of Fig. 4.6 than in the regular conditions of Fig. 4.5. Noise appears to push the value of \dot{z} towards the deterministic value obtained under smoothing. The significant random fluctuations are a result of the noise amplitude needing to be large to dampen the erratic variations in Fig. 4.5.

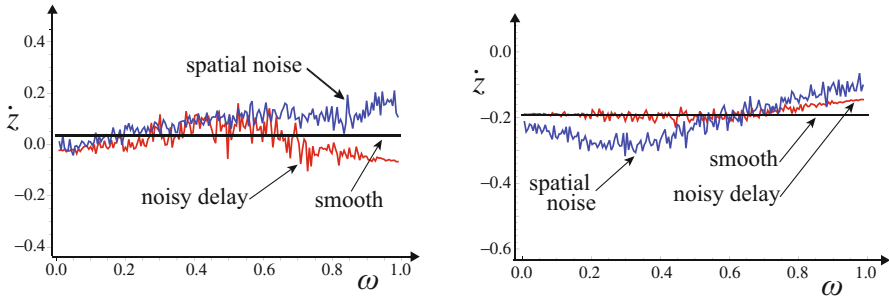


Fig. 4.6 Noisy implementations corresponding to Fig. 4.5

In Sects. 4.1 and 4.2 the implementation could push a system between two different possible behaviours. Here we see a wide range of erratically varying behaviours, and not only do different implementations select entirely different outcomes from within this set, but changing the parameters of the implementation itself, even slightly, selects vastly different behaviours. Different aspects of these rather striking results began emerging across a number of investigations [5, 6, 78, 84]. The erratic and sensitive dependence in the case of hysteresis was first studied in [6], and extended to other implementations in [84], contrasting with the more regular and predictable dynamics resulting from smoothing [5, 78].

The issues involved in the practical modelling of discontinuities clearly involve a number of factors. To begin addressing them we first need a qualitative way to characterize such behaviour, to which we turn now.